Miller, C. (1983a) *Physiol. Rev. 63*, 1209–1242.
Miller, C. (1983b) *Comments Mol. Cell. Biophys. 1*, 413–428.
Miller, C. (1984) *Annu. Rev. Physiol. 46*, 549–558.
Mishina, M., Takai, T., Imoto, K., Noda, M., Takahashi, T., Numa, S., Methfessel, C., & Sakmann, B. (1986) *Nature 321*, 406–411.
Montal, M., Darzon, A., & Schindler, H. (1981) *Q. Rev. Biophys. 14*, 1–79.
Mueller, P., & Rudin, D. O. (1968) in *Laboratory Techniques in Membrane Biophysics* (Passow, R., & Stampfli, E., Eds.) pp 141–156, Springer-Verlag, Berlin.
Mueller, P., Chien, T. F., & Rudy, B. (1983) *Biophys. J. 44*, 375–381.
Nelson, N., Anholt, R., Lindstrom, J., & Montal, M. (1980) *Proc. Natl. Acad. Sci. U.S.A. 77*, 3057–3061.
Popot, J. L., & Changeux, J. P. (1984) *Physiol. Rev. 64*, 1162–1239.
Ravdin, P., & Axelrod, D. (1977) *Anal. Biochem. 80*, 585–592.
Sakmann, B., Methfessel, C., Mishina, M, Takahashi, T., Takai, T., Kurasaki, M., Fukuda, K., & Numa, S. (1985) *Nature 318*, 538–543.
Schindler, H. (1980) *FEBS Lett. 122*, 77–79.
Schindler, H., & Quast. U. (1980) *Proc. Natl. Acad. Sci. U.S.A. 77*, 3052–3056.
Suarez-Isla, B. A., Wan, K., Lindstrom, J., & Montal, M. (1983) *Biochemistry 22*, 2319–2323.
Schmidt, J., & Raftery, M. A. (1973) *Anal. Biochem. 52*, 349–354.
Tank, D. W., & Miller, C. (1983) in *Single Channel Recording* (Sakmann, B., & Neher, E., Eds.) pp 91–105, Plenum Press, New York.
Tank, D. W., Huganir, R. L., Greengard, P., & Webb, W. W. (1983) *Proc. Natl. Acad. Sci. U.S.A. 80*, 5129–5133.

Effect of Unsaturated Phosphatidylethanolamine on the Chain Order Profile of Bilayers at the Onset of the Hexagonal Phase Transition. A ^{2}H NMR Study†

David B. Fenske,‡ Harold C. Jarrell,‡ Yuqing Guo,§ and Sek Wen Hui*,§

Division of Biological Sciences, National Research Council of Canada, Ottawa, Ontario, Canada K1A 0R6, and Membrane Biophysics Laboratory, Roswell Park Memorial Institute, Buffalo, New York 14263

Received March 19, 1990; Revised Manuscript Received August 22, 1990

ABSTRACT: The quadrupolar splitting profiles of methylene groups along the acyl chains of perdeuteriated dimyristoylphosphatidylcholine (DMPC-d_{54}) in mixtures with dioleoylphosphatidylethanolamine (DOPE) were studied by ^{2}H NMR. The quadrupolar splittings, obtained for lipid mixtures in the bilayer state, were measured as functions of temperature and PE:PC ratio and were used to obtain the approximate gauche probabilities at a given chain position, p_B. Ratios (R) of p_B for C13, C12, and C11 relative to that of the plateau region were used to characterize the effect of increasing PE on the gauche content of PC chains. At all temperatures studied (including the bilayer to hexagonal phase transition region), for each ratio R (e.g., $R_{C13/P}$), the relative gauche content of the DMPC chains was similar over the range of 25–85% PE. DOPE is viewed in simple terms as having a "conical" shape; if this geometry applies to the acyl chain region of the molecule, a greater lateral pressure would be expected toward the center of the bilayer as the PE content is increased, resulting in a decreased gauche content, relative to the plateau, of those methylene groups of PC. The failure to observe the predicted increase in lateral pressure has ramifications for the cone-shape molecular model. The overall "cone shape" of PE is seen to arise from the smaller size of the head-group relative to the acyl chains; however, the acyl chain region itself is not rigidly cone-shaped and is better represented by a flexible "balloon". These results were supported by small-angle X-ray diffraction, which showed a decreasing trend in the area per molecule with increasing PE content.

All biological membranes contain some phospholipids that, when isolated, will adopt nonbilayer structures under physiological conditions. The function of these lipids in membranes is not well understood, but it is believed that they help to maintain the membranes at a marginally stable state in order to optimize their functional condition (Wieslander et al., 1986). Many biological membranes, especially the highly active ones such as the inner mitochondrial membranes, the membranes of the photoreceptors, and the thylakoid membranes, have a high content of non-bilayer-preferring lipids. However, none of the biological membranes express the nonbilayer form which would destroy their ability to function as compartmental barriers.

The preference of some lipids for a nonbilayer state is usually viewed in terms of the geometric shape of these lipid molecules. The self-assembly theory of lipid aggregates (Israelachvili et al., 1976, 1980), based on the concept of geometric parameter or "molecular shape", has been widely used to interpret the lipid polymorphism (Cullis & De Kruijff, 1979; Rilfors et al., 1984). Most non-bilayer-preferring lipids, when not otherwise constrained, have unequal cross-sectional areas at the hydrophilic and hydrophobic ends (the *cone-shape* molecular model). Packing of these lipids in a planar bilayer is not energetically favorable as they prefer structures of finite

† This work was supported by Grant GM-28120 (to S.W.H.) from the National Institutes of Health, USPHS.
* Author to whom correspondence should be addressed.
‡ National Research Council of Canada.
§ Roswell Park Memorial Institute.

0006-2960/90/0429-11222$02.50/0

curvature. The energetically preferred curvatures (spontaneous curvatures) can be estimated by the molecular compositions and physicochemical properties of these lipids (Hui & Sen, 1989). The spontaneous curvature can also be deduced from the dimension of the hexagonal phase (Gruner, 1985). The packing of nonbilayer lipids in a bilayer state results in a decrease in bilayer stability, and thus may be thought of as adding energy to the membrane. This extra energy may be expressed as bending energy, which is the highest at the onset of the bilayer to nonbilayer (e.g., hexagonal or cubic) phase transition (Hui & Sen, 1989). A model describing the bending energy of a spontaneously curved monolayer is to treat each monolayer as a pair of attached elastic strips. The outer one is adjacent to the hydrophilic surface and the inner one adjacent to the bilayer center. Each layer has its own elastic modulus and experiences either tension or compression when it is constrained to a plane (Deuling et al., 1976). The molecular motion along the acyl chain is expected to reflect the asymmetric lateral tension across the monolayer.

Deuterium nuclear magnetic resonance (^{2}H NMR) is a proven, nonperturbing technique which provides quantitative information on the local order of acyl chains in phospholipid model membranes (Seelig, 1977). Previous ^{2}H NMR studies (Marsh et al., 1983; Perly et al., 1985; Cullis et al., 1986) have shown that the order parameter in phosphatidylethanolamine (PE)[1] bilayers is higher than in corresponding phosphatidylcholine (PC) bilayers due to the smaller head-group of PE, which may lead to a stronger lateral compression in the hydrocarbon chain region (Perly et al., 1985). The above experiments were carried out with either pure PE or pure PC systems, or with only a few deuteriated positions at a few temperatures. With these limited data, it is not possible to rigorously test the "cone-shape" molecular model which predicts a higher lateral pressure at the hydrophobic core than at the head-group end of the acyl chains, if unsaturated PE is constrained to a bilayer form. In order to clarify this issue, more labeled sites need to be studied in a number of lipid mixture of varying PE composition at the onset and over the whole range of the bilayer to hexagonal phase transition. In the present work, we use perdeuteriated lipid samples to probe the quadrupolar splittings of the acyl chains of DMPC molecules in DMPC/DOPE mixtures. The quadrupolar splitting $\Delta\nu_Q$, which is directly related to the C–^{2}H bond order parameter, was systematically measured as a function of increasing DOPE content and as a function of increasing temperature. ^{2}H NMR provides us with a direct measure of acyl chain order which is sensitive to the putative lateral compression and tension, thereby allowing us to test the geometric packing hypothesis.

In addition, we have also applied small-angle X-ray diffraction to PE/PC mixtures to obtain measurements on bilayer thickness and area per lipid molecule. The data provide additional structural information which enables us to suggest an alternative model for molecular packing.

Materials and Methods

Dioleoyl-PE (DOPE), dioleoyl-PC (DOPC), and perdeuteriated DMPC (DMPC-d_{54}) were purchased from Avanti Polar Lipids, Inc. (Birmingham, AL), and were used without further purification. For the preparation of NMR samples, DMPC-d_{54} (8 mg) and DOPE in chloroform were mixed to the desired ratios and dried under a stream of nitrogen and then under vacuum for at least 1 h. Excess deuterium-depleted water was added to the lipid which was then subjected to several cycles (usually 5) of vortex–freeze–thaw.

4,4-$^2H_2$- and 11,11-$^2H_2$-deuteriated myristic acids were generous gifts from A. P. Tulloch. Selectivity deuteriated DMPCs were synthesized by the methods of Gupta et al. (1977) and Perly et al. (1983). Each NMR sample contained about 6–8 mg of specifically deuteriated DMPC.

^{2}H NMR spectra were acquired at 30.7 MHz as described previously (Jarrell et al., 1986). Spectra were recorded by using the quadrupolar echo pulse sequence (Davis et al., 1976) with full phase cycling (Perly et al., 1985) and quadrature detection. The $\pi/2$ pulse length was 2.4 μs (5-mm solenoid coil), the pulse spacing was 60 μs, and the recycle time was 800 ms. The frequency of the spectrometer was carefully set at the center of the quadrupolar powder patterns. The samples were equilibrated at a given temperature for 20 min prior to data acquisition; temperatures are accurate to ±0.5 °C. The spectra of perdeuteriated DMPC in DOPE were not folded about the Larmor frequency, whereas the spectra of selectively deuteriated DMPC were folded to increase S/N. No spectral distortions were introduced by the folding procedure. Quadrupolar splittings were measured from the 90° oriented sample ("dePaked") spectra which were calculated from the powder spectra as described previously (Bloom et al., 1981). Quadrupolar splitting assignments were based on those of Oldfield et al. (1978) and Davis (1979), and by comparison with selectively deuteriated samples.

For X-ray diffraction studies, the samples were prepared in thin-walled glass X-ray capillaries. About 5–8 mg of lipids (DOPC/DOPE mixtures) in chloroform was added to capillaries and then placed under vacuum for at least 3 h. Samples were returned to atmospheric pressure under N_2 and weighed immediately. For fully hydrated samples, an appropriate amount of distilled water was added by microsyringe, and the capillaries were reweighed, then sealed by silicon "sealant", and equilibrated for at least 1 day at room temperature. For the samples with various degrees of low hydration, the capillaries with dried lipid layers were equilibrated in different relative humidities of 32–98% in sealed containers containing various saturated salt solutions at room temperature for 3–7 days, until the expected degrees of hydration were achieved.

The X-ray diffraction experiments were performed by using a Rigaku rotating-anode X-ray generator and a Frank-type camera. The diffraction patterns were recorded either with a TEC position-sensitive detector or on X-ray films (Kodak, DEF5). The relative intensities for diffraction orders on films were obtained by scanning with a double-beam microdensitometer (Joyce-Loebl Model MK III C).

Phase assignments of diffracting orders were made by the swelling method previously described (Hui & Huang, 1986). The Fourier transform gives the relative electron density profile for each sample. The bilayer thickness, d_B, was measured directly from the peak separation in the electron density profile (McIntosh & Simon, 1986). The area per molecule, S, was calculated by the formula (Luzzati, 1968)

$$S = 2Mv_L/d_BN_A$$

where M is the lipid molecular weight, v_L is the partial specific volume of the lipids, and N_A is Avogadro's number.

Results

Perdeuteriated DMPC was used as a probe for the order parameter of mixed DMPC/DOPE bilayers in the liquid-crystalline L_α state. Five mixtures were examined, corresponding to compositions of 25%, 40%, 60%, 75%, and 85%

[1] Abbreviations: DMPC, dimyristoylphosphatidylcholine; DOPE, dioleoylphosphatidylethanolamine; DOPC, dioleoylphosphatidylcholine; PC, phosphatidylcholine; PE, phosphatidylethanolamine.

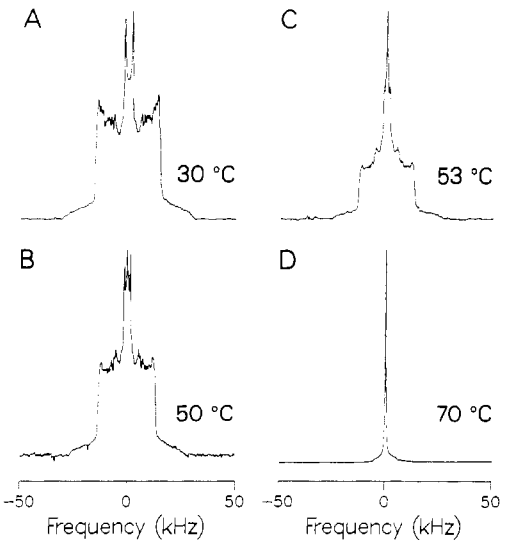

FIGURE 1: ^2H NMR spectra of DOPE/DMPC-d_{54} mixtures at 30.7 MHz: (A) 25% PE at 30 °C; (B–D) 85% PE at 50, 53, and 70 °C, respectively.

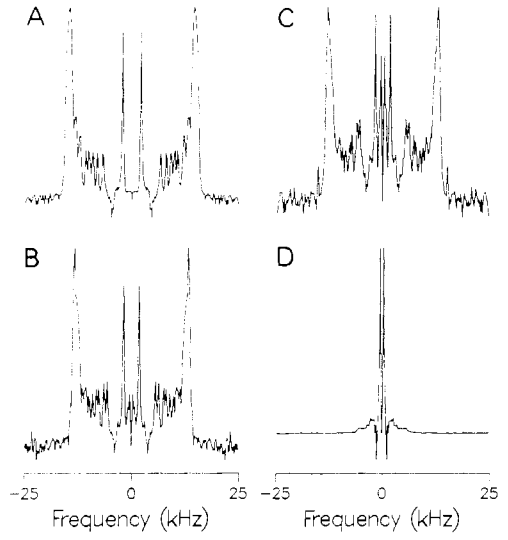

FIGURE 2: DePaked spectra of the corresponding spectra in Figure 1.

PE (by weight). Typical ^2H NMR spectra are shown in Figure 1, and the corresponding 90° oriented sample spectra (de-Paked) are shown in Figure 2. The samples were studied at increasing temperatures from 25 to 70 °C in 5 °C intervals (usually), following which the samples were cooled to 25 °C and the spectra were again recorded. The difference in the spectra before and after heating was minimal for the 25%, 40%, and 60% PE samples, which did not undergo a lamellar to hexagonal phase transition. The lamellar to hexagonal/isotropic phase transition of the 75% and 85% PE samples occurred at approximately 60 and 50 °C, respectively, and these samples remained isotropic upon cooling. Figure 1A shows the spectrum of the lamellar 25% PE sample at a temperature of 30 °C. Spectra of lipid at the onset of the hexagonal phase transition (85% PE at 50 °C), just past the onset of the hexagonal phase transition (85% PE at 53 °C), and in the hexagonal/isotropic phase (85% PE at 70 °C) are shown in panels B, C, and D, respectively, of Figure 1, and the corresponding dePaked spectra are shown in panels B, C, and D of Figure 2. The presence of hexagonal phase lipid is most clearly seen by comparison of panels A and C of Figure 1 panels A and C of Figure 2, where the increase in intensity

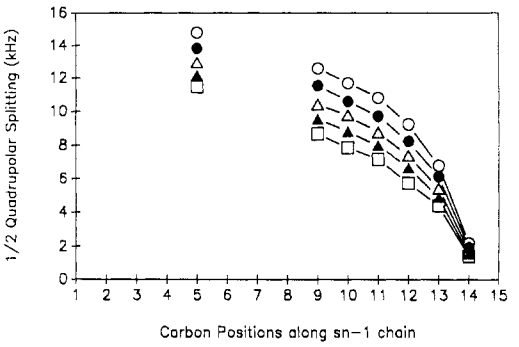

FIGURE 3: Quadrupolar splitting profiles for the *sn*-1 acyl chain of DMPC-d_{54} of a DMPC/DOPE mixture containing 60% PE at the individual temperatures: 30 °C (○); 40 °C (●); 50 °C (△); 60 °C (▲); 70 °C (□). The data points at the C5 position represent the average values of C2–C8, which are referred to as the plateau region.

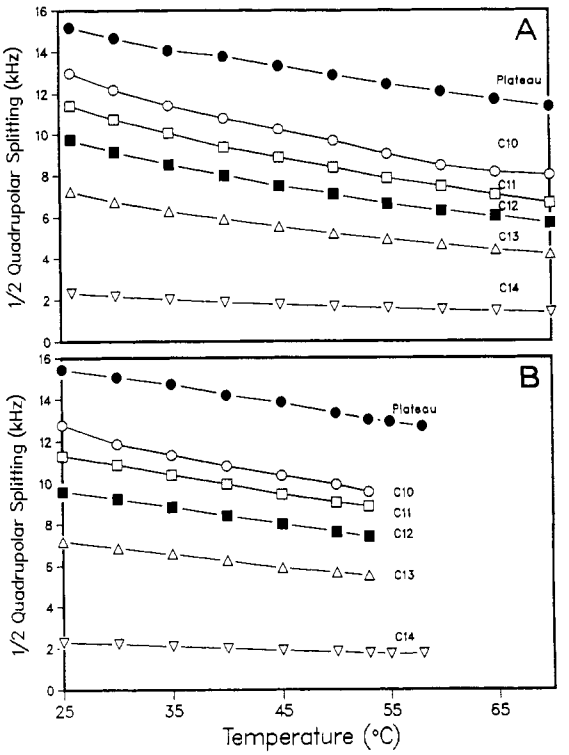

FIGURE 4: Temperature dependences of the quadrupolar splittings of the plateau and C10–C14 deuterons of DMPC-d_{54} (*sn*-1 chain) for (A) 25% PE and (B) 85% PE.

of the innermost splittings flanking the methyl splittings is due to an increase in the plateau region of the hexagonal phase lipid.

An example of the quadrupolar splitting ($\Delta\nu_Q$) profiles for the *sn*-1 chain of perdeuteriated DMPC at different temperatures is shown in Figure 3 for a 60% PE sample. As expected, $\Delta\nu_Q$ is reduced at increasing distance from the head-group. The resonances corresponding to positions C2–C8, which give rise to the characteristic "plateau" region, were not resolvable. Therefore, average values for the "plateau" carbon positions were used in Figure 3. These average values can be determined experimentally within 3% accuracy and also agree to within 3% of that obtained from the [4,4-$^2H_2$]DMPC/DOPE sample (not shown).

As the temperature is increased, the quadrupolar splitting of each position decreases, as shown in Figure 4 for the *sn*-1 plateau C10, C11, C12, C13, and C14 resonances of 25% and 85% PE. Values of $\Delta\nu_Q$ are slightly greater for the 85% PE sample at most temperatures. The rate of decrease in $\Delta\nu_Q$ with

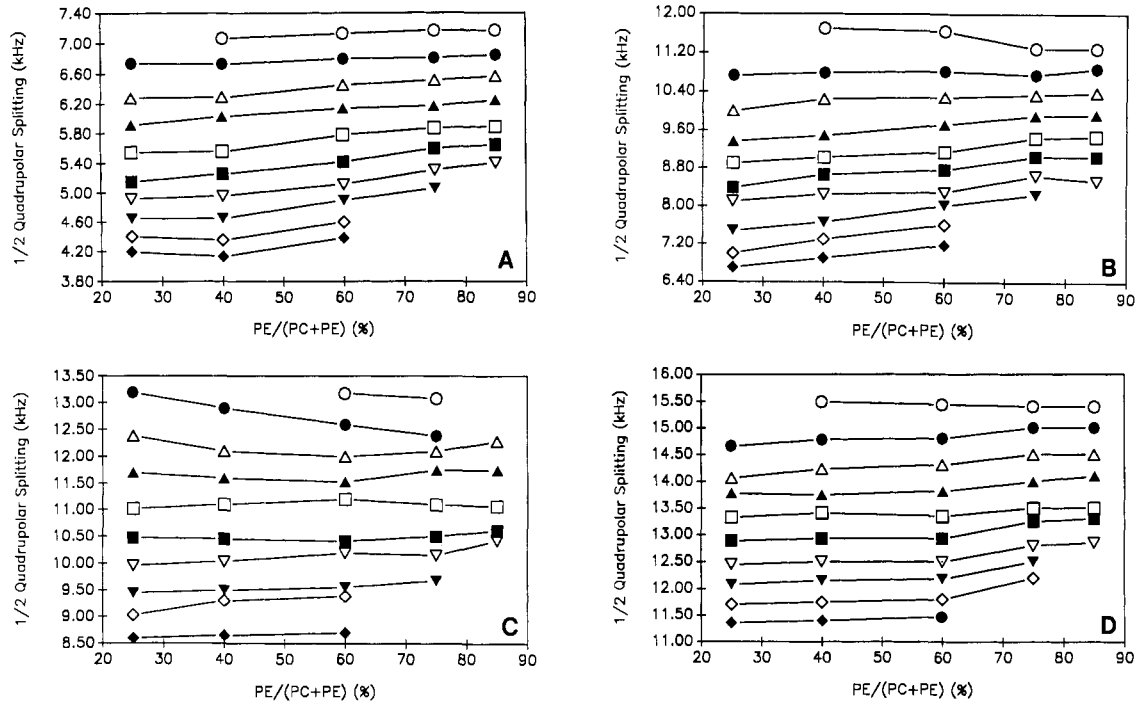

FIGURE 5: Quadrupolar splitting isotherms as a function of percent PE for deuterons at carbon positions (A) C13, (B) C11, and (C) C9 and at the (D) plateau region of DMPC-d_{54}. Symbols represent experimental temperatures at 25 (○), 30 (●), 35 (△), 40 (▲), 45 (□), 50 (■), 55 (▽), 60 (▼), 65 (◇), and 70 °C (◆).

temperature is also slightly reduced for this sample. There is no discontinuity in the lamellar phase plateau and C14 splittings in the mixed phase region where lamellar and hexagonal/isotropic phases coexist, as seen in Figure 4 for the 85% PE plot.

The quadrupolar splittings at each given temperature are compared among samples containing various percentages of DOPE (Figure 5). Isotherms show that at C13 (Figure 5A), next to the methyl terminus, the $\Delta\nu_Q$ values increase slightly with the PE:PC ratio, especially at low temperatures, indicating that the packing difference due to different PE contents has only a weak effect in determining the motional order at this end of the molecule. For C11 and C9 (Figure 5B,C), at low temperatures which are remote from the L_α–H_{II} phase transition temperature, $\Delta\nu_Q$ is observed to decrease as the PE/PC ratio is increased. At higher temperatures, this trend reverses; i.e., $\Delta\nu_Q$ increases with increased PE:PC ratio. For the plateau deuterons (Figure 5D), like most other deuterons, there is no obvious decrease in $\Delta\nu_Q$ with increasing PE even at low temperature.

The geometric parameter model predicts that the acyl chains of PE will possess a cone shape, which may be expected to exert greater lateral pressure on those portions of the PC chains near the methyl terminus. In order to investigate the effects of the putative cone shape of PE on DMPC, we have chosen to examine the changes occurring near the methyl end of the PC acyl chains with the changes occurring at the carboxyl end (the plateau region), as a function of increasing PE content, and to relate this to changes in the gauche content of the acyl chains. The motional freedom of each methylene segment is related to the ability of that segment to undergo trans–gauche isomerization. We have reasoned that the more conical or wedge-shaped the acyl chains, the higher their gauche content, and vice versa. From the measured $\Delta\nu_Q$, one may calculate the parameter p_B, which is approximately the probability of a carbon–carbon bond being in the gauche isomeric state (Seelig & Seelig, 1974):

$$p_B = (1 - S_{mol})/1.125$$

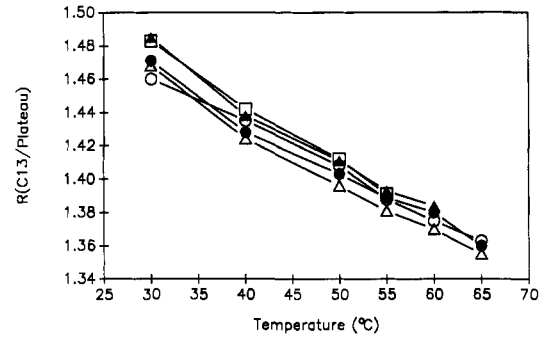

FIGURE 6: Temperature dependence of $R_{C13/P}$ for 25% PE (○), 40% PE (●), 60% PE (△), 75% PE (▲), and 85% PE (□) samples.

where $S_{mol} = -2S_{CD}$, with S_{CD} assumed to be negative. We then express this in terms of $\Delta\nu_Q$ to obtain

$$p_B = \{1 - [8\Delta\nu_Q/3(e^2qQ/h)]\}/1.125$$

The ratios R of p_B of C13–C11, and in some cases C10, to p_B of the plateau (designated as P) were then calculated. Thus, in a plot of $R_{C13/P}$ vs percent PE, an increasing in R implies an increase in the gauche content of C13 relative to the plateau region as the PE content is increased.

Plots of $R_{C13/P}$ vs temperature are shown in Figure 6 for the five mixtures studied. It is clear that as the temperature is increased, there is a decrease in the gauche content of the methyl terminii relative to the plateau for all PE compositions. This probably represents a relative increase in the motional freedom of the plateau positions rather than a decrease in the motional freedom of the methyl terminus. Although the values of $R_{C13/P}$ are slightly higher for the 75% and 85% PE samples, suggesting slightly more gauche content at these compositions, the increase is not significant compared to the uncertainty in the ratio (about ±3%). The interesting observation is that the slopes of the plots are approximately the same for all PE compositions. Similar plots are obtained for $R_{C12/P}$ and $R_{C11/P}$ as a function of temperature (not shown). The plot of $R_{C12/P}$

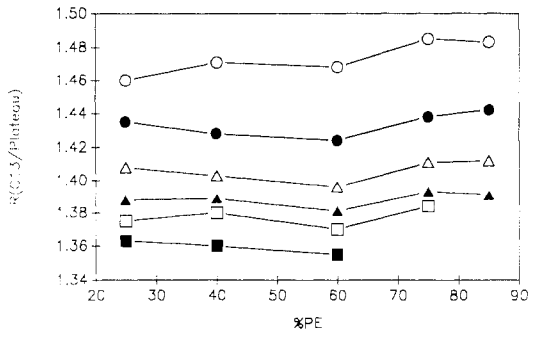

FIGURE 7: $R_{C13/P}$ as a function of percent PE at the indicated temperatures: 30 °C (○); 40 °C (●); 50 °C (△); 55 °C (▲); 60 °C (□); 65 °C (■).

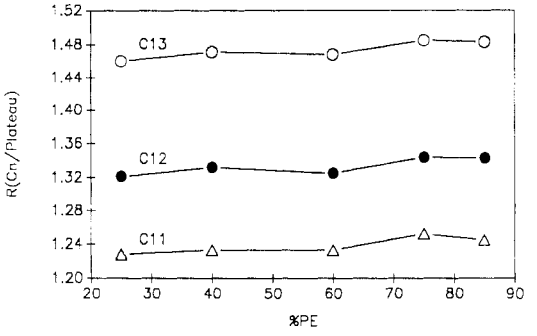

FIGURE 8: Plot of R (for C13, C12, and C11 relative to the plateau) as a function of percent PE at 55 °C.

is essentially identical with that obtained if the data of Oldfield et al. (1978) for pure DMPC are treated in the same manner (not shown).

Plots of $R_{C13/P}$ as a function of percent PE are shown in Figure 7 for several temperatures. There is little change in $R_{C13/P}$ with increasing PE at all temperatures, including the lamellar to hexagonal transition temperatures of the 75% and 85% PE samples. Again, similar plots were obtained for $R_{C12/P}$ and $R_{C11/P}$ as a function of percent PE (not shown).

Further insight can be obtained by plotting several different R's at a given temperature as a function of percent PE. One such plot is presented in Figure 8 for 55 °C. The 55 °C plot is of interest as this temperature is the midpoint of the lamellar to hexagonal phase transition temperatures of the 75% and 85% PE samples. At this temperature, the values of $R_{C13/P}$, $R_{C12/P}$, and $R_{C11/P}$ are all roughly constant with increasing PE. The plots for other temperatures (not shown) are very similar to those observed at 55 °C.

For purposes of comparison, $\Delta\nu_Q$ data obtained from pure DMPC multilamellar dispersions (Oldfield et al., 1978) and from 1-palmitoyl-2-[16,16-$^2H_2$]oleoyl-PE multilamellar dispersions (B. Perly and H. C. Jarrell, unpublished results) were expressed as R values (data not shown). The plots for pure DMPC were similar to those presented here. For POPE, a plot of $R_{C16/C5}$ shows only a slight monotonic decrease with temperature, even in the range 55–70 °C where lamellar and hexagonal phase coexist. Thus, for a pure PE sample, there is no change in R at the onset of the lamellar to hexagonal transition, nor in the mixed phase region.

In order to gain more insight into the molecular packing of PE with PC, X-ray diffraction was used to measure the bilayer thickness and area per molecule at increasing DOPE:DOPC ratio. DOPC was used to ensure that the measured structural changes with increasing PE can be attributed to the head-groups alone. An example of an X-ray diffraction pattern is shown in Figure 9 (DOPE:DOPC ratio

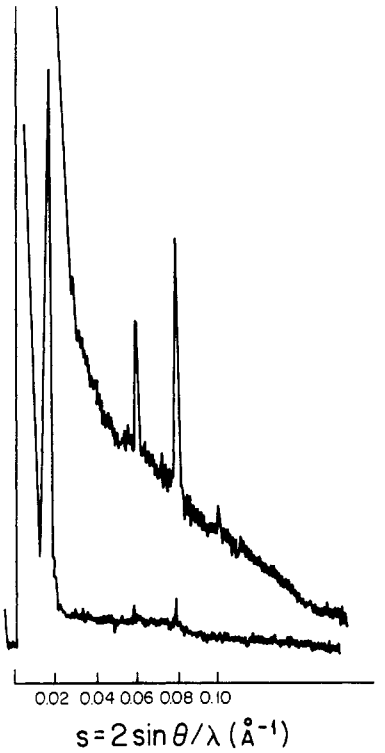

FIGURE 9: X-ray diffraction pattern of a sample of DOPE/DOPC (7:3) with 13.5% water. The upper trace is a more sensitive scan of the same film.

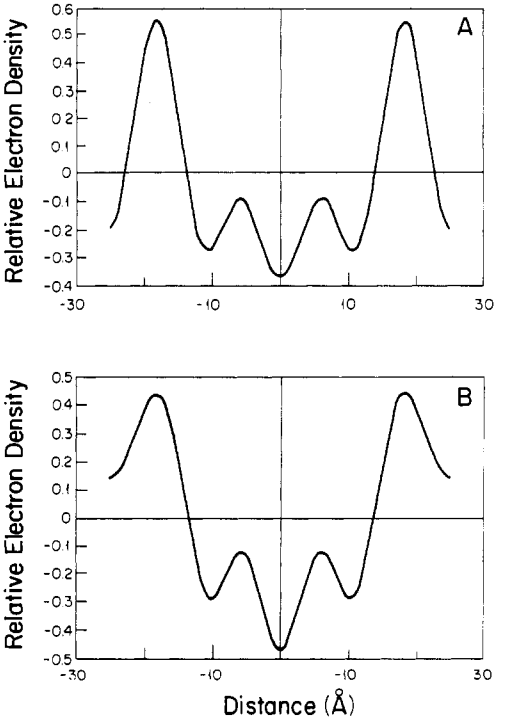

FIGURE 10: Electron density profiles for (A) pure DOPC and (B) DOPE/DOPC (7:3) bilayers.

Table I: Bilayer Thickness and Area per Molecule of Lipid Mixtures as Given by X-ray Diffraction Measurements

lipid	d_B (Å)	S (Å^2)
DOPC	36 ± 1	72 ± 3
	36 ± 2[a]	70 ± 4[a]
DOPE/DOPC (7:3)	37 ± 1	67 ± 3
DOPE	37 ± 3[a]	65 ± 5[a]

[a] Data from Gruner et al. (1988).

of 7:3, 13.5% water), in which five diffraction orders can be seen. By the swelling method, their phases were assigned as π, π, 0, π, and π, respectively. In Figure 10, two electron density profiles for pure DOPC and DOPE/DOPC (7:3) are compared. The bilayer thickness and area per lipid molecule (mean ± SD, $N = 4$ experiments) are listed in Table I. The DOPC measurement agrees with that obtained by Gruner et al. (1988) using the Luzzati method. The bilayer thickness, d_B, shows little change with different lipid compositions. The decreasing trend in the area per molecule with PE content agrees with Gruner et al. (1988) and with Rand and Parsegian (1989). We expect that this trend also applies to DOPE/DMPC mixtures.

Discussion

The aim of this work is to test if there is a detectable change in the lateral pressure along the acyl chain when "cone-shaped" molecules such as unsaturated PE are added to the bilayer. According to the self-assembly theory of lipid aggregates (Israelachvili et al., 1976, 1980), the structure assumed by aqueous lipid dispersions can be associated with a geometric parameter (P):

$$P = V/al_c$$

where V is the hydrocarbon chain volume, a is the hydrocarbon–water interfacial area associated with the lipid, and l_c is the hydrocarbon chain length. When $P > 1$, as is the case for most PE's, inverted hexagonal structures are obtained. Note that in order for this condition to hold, the actual hydrocarbon chain volume must exceed the cylinder volume al_c, indicating a cone shape for the acyl chains. It has been shown by ^{2}H NMR that in the hexagonal phase, there is an increase in the allowed angular fluctuations at any acyl chain segment, with the increasing being larger toward the end of the segment (Perly et al., 1985), a finding supported by FT-IR studies (Mantsch et al., 1981). If the acyl chains of PE's also adopt a cone shape in mixed-bilayer systems, one would expect a decrease in the lateral pressure at the plateau, and an increase in the lateral pressure toward the center of the bilayer, where the base of the cone is situated. The ^{2}H NMR quadrupolar splittings, which can be related to the C–^{2}H bond order parameter, and to the gauche content of the labeled methylene group, should reflect these changes in lateral pressure, which would affect the angular freedom of the acyl chains. By comparing the proportion of gauche isomers toward the end of the chain relative to that of the plateau for different PE contents, we should be able to test the applicability of the geometric model to the systems under study.

In order to facilitate interpretation of the data, an estimate of the anticipated change in $\Delta\nu_Q$ resulting from "cone-shaped" DOPE would be useful. The relationship between the order parameter profile and lateral pressure has been modeled by Meraldi and Schlitter (1981). The change in order parameter S_{CD} with lateral pressure varies slightly along the chains, and is averaged to about 0.10 (or 12.8 kHz in terms of $\Delta\nu_Q$) per 18 dyn/cm. The differential pressure along the chain for each geometric model is related to the spontaneous curvature, the bending elastic modulus, and the hypothetical pivot point pertinent to that model. Two possible geometric models are considered here. The cone-shaped model (Figure 11B) assumes a pivot point somewhere between the head-group and the methyl end of the chain. With more "cone-shaped" molecules, such as PE, in the bilayer, the methyl (and C13) end would experience a higher lateral pressure, whereas the positions above the pivot point would experience a lower

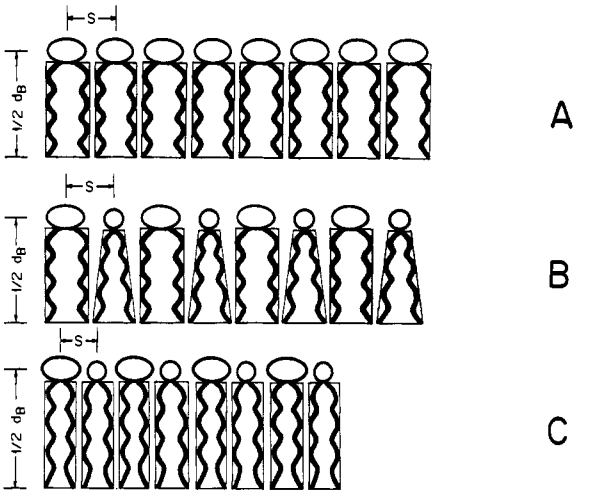

FIGURE 11: Schematic representations of the molecular packing in a bilayer of (A) PC only, (B) PC and "cone-shaped" PE, and (C) PC and PE in a "soft-balloon" model. PC and PE molecules are depicted in their large and small head-groups, respectively.

pressure. The "soft-balloon" model (Figure 11C) is an extreme case of the "cone-shaped" model, in which the pivot point is at or beyond the head-group, such that the entire chain experiences the same lateral pressure change. The increase in lateral pressure is determined by the bending energy, which is proportional to the product of the binding modulus and the square of the spontaneous curvature (Deuling & Helfrich, 1976). The latter quantity may be estimated from the constituent molecules (Hui & Sen, 1989) or by direct measurement (Gruner et al., 1986).

Using the former method, we estimated the spontaneous radii of curvatures of the 60%, 75%, and 85% DOPE samples to be 5.5, 4.4, and 4.0 nm, respectively; 4.4 nm approximately equals the measured spontaneous radius of curvature for DOPE/DOPC (3:1) of 3.8 nm (Rand et al., 1990). The hydrocarbon chains are subjected to an expected total lateral pressure increase of approximately 6.5, 9.9, and 12.7 dyn/cm, respectively, from that of a stable bilayer (Evans & Skalak, 1979). If the pressure is shared equally by the 28 carbons of a DMPC bilayer (Seddon, 1990), as expected for the "soft-balloon" model, each carbon in the 3 mixtures would experience a respective 0.16-, 0.25-, and 0.32-kHz increase in $\Delta\nu_Q$. This represents an increase of 2.5% in C13 and 1.2% in the plateau values (using typical $\Delta\nu_Q$ values of about 12 kHz for C13 and about 27 kHz for the plateau) and a corresponding decrease of 1.5% in $R_{C13/P}$ as the PE content increases from 0% to 85%. For the "cone-shaped" model, on the other hand, if the pivot point is placed at the plateau, and assuming a linear increase in pressure extending to the end of the chain (Seddon, 1990), the $\Delta\nu_Q$ increase in C13 and the corresponding decrease in $R_{C13/P}$ would be 10%. The experimental uncertainty in a given R value is ±3%; thus, the maximum variation in R due to error would be on the order of 6%. This suggests that the two models should be distinguishable, as the change in R anticipated for the cone-shaped model is greater than the experimental uncertainties.

As the PE content is increased from 25 to 85%, the DMPC quadrupolar splittings increase for all positions, indicating that the PE has an ordering effect on the PC. This is consistent with the greater lateral compression or ordering observed in pure POPE bilayers in the liquid-crystalline phase, compared with the POPC analogue, which is due to the smaller area of the PE head-group (Perly et al., 1985). The general increase of 0.3–0.5 kHz in $\Delta\nu_Q$ for all carbon positions with increasing

PE, as the system approaches the hexagonal phase transition, indicates an increase of 0.4–0.7 dyn/cm of lateral pressure throughout the acyl chains. The low-temperature anomaly for C9 and C11 may be attributed to the cis double bonds of DOPE which are located at C9–C10. Their permanent "kinks" may create a defect in this region making it more disordered. This local effect appears to diminish as the temperature increases, when the entire chain experiences a similar degree of increasing lateral compression.

To facilitate interpretation of the data, we have examined the ratios of the gauche probabilities of terminal positions relative to the plateau. In this manner, differential effects at the center of the bilayer should be readily discerned. Plots of $R_{C13/P}$ vs percent PE are shown in Figure 7 for several temperatures between 30 and 65 °C. What is striking is the similarity of the plots at all temperatures. At 30 °C, there is little change (2 ± 3%) in the value of $R_{C13/P}$ as the PE content is increased from 25 to 85%. The addition of PE has little effect upon the gauche content of C13 relative to the plateau in DMPC. On the basis of the cone-shape molecular model, one would predict a decrease in $R_{C13/P}$ with increasing PE; i.e., the presence of more conical PE should result in a greater lateral pressure near the center of the bilayer, which would reduce the motional freedom of the DMPC methyl group relative of the plateau. By the above estimate, the $R_{C13/P}$ value would decrease by a detectable 10%. On the contrary, the "soft-balloon" model would predict a decrease of only 1.5% in $R_{C13/P}$, very close to what is actually observed. Nevertheless, this effect may not be seen at lower temperatures, since the bending energy of nonbilayer lipids such as PE is greatest at the onset of the lamellar to hexagonal phase transition. Thus, the essentially identical curves observed between 50 and 65 °C suggest strongly that the DMPC acyl chains are *not* experiencing a greater lateral pressure at the bilayer center relative to the plateau at higher PE concentrations.

Figure 8 shows the change in R for C13 to C11 as a function of PE content at 55 °C. Similar curves are obtained for all positions. Within experimental uncertainty of ±3%, there is essentially no response by the DMPC to PE contents varying from 25 to 85%, as assessed by the ratios of the gauche probabilities, even at temperatures close to the bilayer to hexagonal transition. This suggests that the PE exerts a uniform lateral pressure variation with temperature on the DMPC acyl chains. The absence of differential lateral pressure variation and the more or less uniform ordering observed along the chain with the introduction of PE imply that, mechanically, the monolayer behaves like an incompressible net of head-groups, where the inflection or pivotal boundary layer should be located, plus a thick, elastic layer extending through the entire hydrocarbon interior. In other words, the molecular packing can be represented by "soft-balloon" acyl chains, which are inflated with increasing temperature (Figure 11C).

Our X-ray diffraction data tend to favor this "soft-balloon" model rather than the "cone-shaped" molecular model. According to the cone-shaped model, which assumes somewhat rigidly shaped molecules, neither d_B nor S will change when PE molecules are added to the PC bilayer (Figure 11B). Instead, there will be an increase in lateral pressure near the bottom, and the creation of more available volume and a decrease in lateral pressure near the smaller head-groups of PE molecules. For the "soft-balloon" model, both PC and PE head-groups are tightly packed, and when further PE molecules are added to the bilayer, the average S will decrease due to the smaller head-group area of PE. The decreasing trend in S is indicated by our X-ray diffraction data and those from Gruner et al. (1988) and from Rand and Parsegian (1989).

Our results allow a refinement of the geometric-shape packing model. It is clear that PE does not induce in its neighbors a greater lateral compression toward the center of the bilayer than at the interfacial region. Hence, the cone shape of PE, which has been used to explain its preference for the inverted hexagonal phase, must be understood in terms of the area of the head-group relative to the acyl chains. The acyl chains themselves do not seem to adopt a "rigid" cone geometry in mixtures with DMPC. The formation of nonbilayer structures at higher temperatures is driven by an increased acyl chain volume which, due to the constant head-group volume, would force a finite curvature of the monolayer at the expense of the inter-monolayer interaction. The increased bending energy added to the membrane by non-bilayer-preferring PE is manifest by an increase of lateral pressure over the entire length of the hydrocarbon chain, rather than increasing pressure toward the center of the bilayer, even at the onset of the bilayer to hexagonal phase transition.

ACKNOWLEDGMENTS

We thank A. P. Tulloch for his gift of specifically deuteriated myristic acid. The synthesis of specifically deuteriated DMPC was done by T. Isac. Discussion with A. Sen is appreciated.

Registry No. DMPC, 18194-24-6; DOPE, 2462-63-7.

REFERENCES

Bloom, M., Davis, J. H., & MacKay, A. I. (1981) *Chem. Phys. Lett. 80*, 198–202.

Cullis, P. R., & De Kruijff, B. (1979) *Biochim. Biophys. Acta 559*, 399–420.

Cullis, P. R., Hope, M. J., & Tilcock, C. P. S. (1986) *Chem. Phys. Lipids 40*, 127–144.

Davis, J. H. (1979) *Biophys. J. 27*, 339–358.

Davis, J. H., Jeffrey, K., Bloom, M., Valic, M. I., & Higgs, T. P. (1976) *Chem. Phys. Lett. 42*, 390–394.

Deuling, H. J., & Helfrich, W. (1976) *J. Phys. (Les Ulis, Fr.) 37*, 1335–1339.

Evans, E., & Skalak, A. (1979) *The Mechanics and Thermodynamics of Biomembranes*, CRC Press, Boca Raton, FL.

Gruner, S. M. (1985) *Proc. Natl. Acad. Sci. U.S.A. 82*, 3665–3669.

Gruner, S. M., Parsegian, V. A., & Rand, R. P. (1986) *Faraday Discuss. Chem. Soc. 81*, 29–37.

Gruner, S. M., Tate, M. W., Kirk, G. L., So, P. T. C., Turner, D. C., Keane, D. T., Tilcock, C. P. S., & Cullis, P. R. (1988) *Biochemistry 27*, 2853–2866.

Gupta, C. M., Radhakrishnan, R., & Khorana, H. G. (1977) *Proc. Natl. Acad. Sci. U.S.A. 74*, 4315–4319.

Hui, S. W., & Huang, C. H. (1986) *Biochemistry 25*, 1330–1335.

Hui, S. W., & Sen, A. (1989) *Proc. Natl. Acad. Sci. U.S.A. 86*, 5825–5829.

Israelachvili, J. N., Mitchell, D. J., & Ninham, B. W. (1976) *J. Chem. Soc., Faraday Trans. 2, 72*, 1525.

Israelachvili, J. N., Marcelja, S., & Horn, R. G. (1980) *Q. Rev. Biophys. 13*, 121–200.

Jarrell, H. C., Giziewicz, J. B., & Smith, I. C. P. (1986) *Biochemistry 25*, 3950–3957.

Luzzati, V. (1968) in *Biological Membranes, Physical Fact and Function* (Chapman, D., Ed.) pp 71–123, Academic Press, New York.

Mantsch, H. H., Martin, A., & Cameron, D. G. (1981) *Biochemistry 20*, 3138–3145.
Marsh, D., Watts, A., & Smith, I. C. P. (1983) *Biochemsitry 22*, 3023–3026.
McIntosh, T. J., & Simon, S. A. (1986) *Biochemistry 25*, 4948–4952.
Meraldi, J.-P., & Schlitter, J. (1981) *Biochim. Biophys. Acta 645*, 193–210.
Oldfield, E., Meadows, M., Rice, D., & Jacobs, R. (1978) *Biochemistry 17*, 2727–2740.
Perly, B., Dufourc, E. J., & Jarrell, H. C. (1983) *J. Labelled Compd. Radiopharm. 21*, 1–13.
Perly, B., Smith, I. C. P., & Jarrell, H. C. (1985) *Biochemistry 24*, 1055–1063.
Rand, R. P., & Parsegian, V. A. (1989) *Biochim. Biophys. Acta 988*, 351–376.
Rand, R. P., Fuller, N. L., Gruner, S. M., & Parsegian, V. A. (1990) *Biochemistry 29*, 76–87.
Rilfors, L., Lindblom, G., & Wieslander, A. (1984) in *Membrane Fluidity, Biomembranes* (Kates, M., & Manson, L. A., Eds.) Vol. 12, pp 205–245, Plenum Press, New York and London.
Seddon, J. M. (1990) *Biochim. Biophys. Acta 1031*, 1–69.
Seelig, J. (1977) *Q. Rev. Biophys. 10*, 353–418.
Seelig, A., & Seelig, J. (1974) *Biochemistry 13*, 4839–4845.
Wieslander, A., Rilfors, L., & Lindblom, G. (1986) *Biochemistry 25*, 7511–7517.

Interaction of Chondroitin Sulfate with Perforin and Granzymes of Cytolytic T-Cells Is Dependent on pH†

Daniele Masson,*,‡ Peter J. Peters,§ Hans J. Geuze,§ Jannie Borst,‖ and Jürg Tschopp‡

Institute of Biochemistry, University of Lausanne, Chemin des Boveresses 155, CH-1066 Epalinges, Switzerland, Faculty of Medicine, Department of Cell Biology, University of Utrecht, Utrecht, The Netherlands, and Department of Immunology, The Netherlands Cancer Institute, Amsterdam, The Netherlands

Received February 22, 1990; Revised Manuscript Received August 23, 1990

ABSTRACT: Cytolytic T-lymphocytes (CTL) harbor cytoplasmic granules containing the lytic, pore-forming protein perforin, a family of serine proteases designated granzymes, and proteoglycans as major constituents. Growth of CTL lines in the presence of PNP-xyloside completely inhibited the glycosylation of the granule-associated chrondroitin sulfate A type proteoglycans. Only short glycosaminoglycan molecules were detected. The absence of intact proteoglycans neither altered the sorting of the granule-associated proteins perforin or granzyme A nor influenced their secretion into the extracellular milieu upon T-cell receptor complex stimulation. With a weak base, the pH of the granules was determined to be acidic. At pH 5.2, granzyme A and perforin formed complexes with chondroitin sulfate A. At neutral pH, perforin and only a minor fraction of granzyme A dissociated from the proteoglycan. Upon secretion of the granule contents induced by immobilized anti-CD3 antibodies, most granzyme A molecules remained complexed with the chondroitin sulfate A glycosaminoglycans, even if synthesis of intact proteoglycans was inhibited. We suggest that granule-associated molecules complex with proteoglycans under the acidic conditions prevailing in the trans Golgi and cytolytic granules. A possible pH shift occurring during exocytosis would cause perforin, but only a minor fraction of granzyme A, to dissociate from the proteoglycans.

Cytotoxic T-lymphocytes (CTL) and natural killer (NK) cells contain characteristic electron-dense granules in the cytoplasm. One of the mechanisms of target cell lysis would involve the release of the granule content into the intercellular space between CTL and the target cell upon specific target recognition (Henkart, 1985; Müller-Eberhard, 1988; Podack, 1986; Tschopp & Jongeneel, 1988; Young et al., 1988). Several molecules contained in the granules have been characterized: (1) perforin, a cytolytic protein known to polymerize in the presence of Ca^{2+} into poly(C9)-like tubules on the target cell membrane, thereby rendering it leaky (Masson & Tschopp, 1985; Podack et al., 1985); (2) granzymes, serine esterases with unknown function (Pasternack et al., 1986; Simon et al., 1986; Young et al., 1986a; Masson & Tschopp, 1987); (3) proteoglycans of the chondroitin sulfate A type (MacDermott et al., 1987; Parmley et al., 1985; Stevens et al., 1987). Granzyme A (Pasternack & Eisen, 1985; Takayama & Sitkovsky, 1987; Garcia-Sanz et al., 1987), granzyme B (Jenne & Tschopp, 1988), granzyme D, and proteoglycans (Schmidt et al., 1985) have been detected in the medium during cytolytic assays, indicative of a secretory process.

Other effector cells also participating in the immune response have secretory granules. In particular, mast cells of both the connective tissue and mucosal type harbor proteoglycans and proteases in their intracellular granules (Stevens et al., 1986; Avraham, 1989). Proteoglycans including heparin, heparan sulfate, and chondroitin sulfate consist of long unbranched sulfated polysaccharide chains composed of repeating disaccharide units bound to a core protein. The peptide core contains clusters of alternating serines and glycines (Bourdon et al., 1985). Glycosaminoglycans are attached via an O-

† This work was supported by grants from the Swiss National Science Foundation (to J.T.) and the Netherlands Organization for Scientific Research (Grant H93-155 to J.B.).
* Address correspondence to this author.
‡ University of Lausanne.
§ University of Utrecht.
‖ The Netherlands Cancer Institute.

0006-2960/90/0429-11229$02.50/0